

Exploring preserved fossil dinoflagellate and haptophyte DNA signatures to infer ecological and environmental changes during deposition of sapropel S1 in the eastern Mediterranean

Arjan C. Boere,¹ W. Irene C. Rijpstra,¹ Gert J. de Lange,² Elisa Malinverno,³ Jaap S. Sinninghe Damsté,^{1,2} and Marco J. L. Coolen^{1,4}

Received 16 February 2010; revised 7 January 2011; accepted 25 January 2011; published 16 April 2011.

[1] In this study we used a comparative multiproxy survey (fossil DNA, calcareous nannofossils, and lipid biomarkers) to test whether preserved genetic signatures provide an accurate view of haptophyte and dinoflagellate populations during deposition of the eastern Mediterranean sapropel S1 and the organic carbon-depleted oxidized marls flanking the S1 and to see if we could identify important environmental indicator species that did not fossilize and escaped previous microscopic identification. The marls above and below the S1 contained low concentrations of lipid biomarkers diagnostic for dinoflagellates and haptophytes (i.e., dinosterol and long-chain alkenones), but 500 base pair long ribosomal DNA fragments of these protists were below the detection limit. In contrast, dinoflagellate and haptophyte DNA could be recovered from the organic carbon-rich S1, but the most abundant sequences did not represent species that were part of the nannofossil (this study) or previously described dinocyst composition. The oldest section of S1 (9.8 to ~8 ¹⁴C kyr B.P.) revealed a predominance of dinoflagellate phylotypes, which were previously only detected in anoxic Black Sea sediments. In the same section of the core, the most abundant haptophyte sequence showed highest similarity with uncultivated haptophytes that were previously shown to grow mixotrophically as predators of picocyanobacteria, an adaptation that promotes growth in oligotrophic marine waters. Sequences with highest similarities to clones found in marine surface waters predominated in the S1 after ~8 ¹⁴C kyr B.P. We discuss whether the shifts in haptophyte and dinoflagellate populations inferred from the preserved DNA reflect known environmental changes that occurred during the formation of sapropel S1.

Citation: Boere, A. C., W. I. C. Rijpstra, G. J. de Lange, E. Malinverno, J. S. Sinninghe Damsté, and M. J. L. Coolen (2011), Exploring preserved fossil dinoflagellate and haptophyte DNA signatures to infer ecological and environmental changes during deposition of sapropel S1 in the eastern Mediterranean, *Paleoceanography*, 26, PA2204, doi:10.1029/2010PA001948.

1. Introduction

[2] The geological record offers our best opportunity for understanding how biological systems function over long timescales and under varying paleoenvironmental conditions. Understanding these ecosystem responses to change is critical for biologists in trying to understand how organisms interact and adapt to environmental changes, and for geologists seeking to use these biology-geology relationships in

order to reconstruct past climate conditions from sediment records. For example, enumeration of microscopic fossilizing calcareous and silicifying protists has become a standard paleoecological approach in the field of paleoclimatology [Castradori, 1993; Meier *et al.*, 2004; Zonneveld *et al.*, 2008]. However, the identification of morphological remains is not always straightforward, as many taxa lack diagnostic features preserved upon fossilization. For example, dinocysts are not produced by all dinoflagellate species, they can be preferentially degraded in the sediment and in many cases, fossil cysts cannot be linked to those of extant species [Boere *et al.*, 2009; Head, 1996; Zonneveld *et al.*, 2008]. Likewise, nannofossils of calcareous haptophytes serve as paleo-environmental proxies, but many important taxa do not calcify [Coolen *et al.*, 2004b; Edvardsen *et al.*, 2000], or species produce coccoliths only during some phases of their life cycle [i.e., Frada *et al.*, 2006] and cannot be identified from a micropaleontological approach. Lipid-based records can be particularly valuable in the absence of diagnostic cellular

¹Department of Marine Organic Biogeochemistry, NIOZ Royal Netherlands Institute for Sea Research, Den Burg, Netherlands.

²Faculty of Earth Sciences, Utrecht University, Utrecht, Netherlands.

³Department of Geological Sciences and Geotechnologies, University of Milan-Bicocca, Milan, Italy.

⁴Department of Marine Chemistry and Geochemistry, Woods Hole Oceanographic Institution, Woods Hole, Massachusetts, USA.

features in the sedimentary record. Nevertheless, the interpretation of these molecular stratigraphic records is often complicated by the limited specificity of many lipid biomarkers [Volkman *et al.*, 1998; Volkman, 2003]. For instance, dinosterol is widely used to estimate the relative dinoflagellate contribution to sedimentary organic matter (OM) and for reconstructing paleoenvironmental conditions [Boon *et al.*, 1979; Robinson *et al.*, 1984; Volkman *et al.*, 1998], although there are important quantitative differences between dinosterol and dinocyst data [Mouradian *et al.*, 2007; Sangiorgi *et al.*, 2005]. In addition, haptophyte-specific lipid biomarkers (long-chain alkenones) are of great interest to paleoceanographers because of the strong empirical relationship between the degree of unsaturation in alkenones (U_{37}^k -unsaturation parameter) and growth temperature, which forms the basis for their use as a molecular proxy of past sea surface temperatures (SSTs) [e.g., Brassell *et al.*, 1986; Prahl and Wakeham, 1987]. However, identification of fossil sources for species-specific calibration of alkenone-inferred SST values [e.g., Versteegh *et al.*, 2001] is not always straightforward as both calcifying (*Emiliania huxleyi* and *Gephyrocapsa oceanica*) and non-fossilizing species (e.g., *Isochrysis* spp. and *Chrysolita lamellosa*) can be planktonic sources of fossil alkenones [Marlowe *et al.*, 1984; Rontani *et al.*, 2004; Versteegh *et al.*, 2001; Volkman *et al.*, 1995].

[3] There is thus a need for biomarkers with greater source specificity that can be used to complement and enhance interpretations based on existing methods. The field of molecular biology offers a most promising approach that is just starting to gain wider utility: the use of ancient plankton DNA in the sedimentary record, most frequently referred to as fossil DNA, to reconstruct past ecosystems. For example, fossil DNA has been analyzed recently to reconstruct the Holocene succession of planktonic protists (haptophytes, dinoflagellates, diatoms), zooplankton (copepods), and photosynthetic bacterioplankton (cyanobacteria and sulfidic chemocline-derived purple and green sulfur bacteria) in shallow lakes and fjords [Bissett *et al.*, 2005; Coolen *et al.*, 2004a, 2004b, 2006b, 2007, 2008; Coolen and Overmann, 1998; D'Andrea *et al.*, 2006]. Fossil DNA stratigraphy also aided in a better understanding of the Holocene ecology and environmental conditions of the world's largest permanently stratified anoxic basin, the Black Sea [Coolen *et al.*, 2006a, 2009; Manske *et al.*, 2008]. The permanent water column stratification and bottom water anoxia in these settings is generally thought to have enhanced the preservation of DNA in the underlying undisturbed, organic carbon-rich, laminated sediments [Coolen *et al.*, 2006a; Coolen and Overmann, 1998; Corinaldesi *et al.*, 2008]. A major benefit of using fossil genetic signatures as highly specific "biomarkers" is the ability to identify also important paleoenvironmental indicator species that leave no other diagnostic features in the sediment record [Bissett *et al.*, 2005; Boere *et al.*, 2009; Coolen and Overmann, 1998, 2007], and to validate paleoenvironmental information inferred from more traditional proxies [Coolen *et al.*, 2004b, 2009; D'Andrea *et al.*, 2006].

[4] Past eukaryotic phytoplankton and zooplankton species are mainly reconstructed based on preserved ribosomal RNA encoding gene fragments (e.g., 18S rRNA genes or 18S rDNA). Although the 18S rRNA gene is relatively con-

served and different species can carry identical sequences, it is the most frequently used phylogenetic marker for eukaryotes and large public databases are available for sequence similarity comparison. Furthermore, primers can be designed for polymerase chain reaction-based (PCR) assays to target regions of the 18S rRNA that are conserved at different taxonomic levels in order to cover a large variety of species within a group of interest. This feature is important when limited information is available about the past plankton diversity in an environmental setting.

[5] Eastern Mediterranean sapropels are dark sedimentary units with organic carbon (C_{org}) contents of >2 wt% that occur intercalated within C_{org} -poor (~0.2 wt%) pelagic-hemipelagic carbonate oozes [Kidd *et al.*, 1978], and represent a potentially rich, but largely untapped archive for the testing of paleogenetics as a tool to assess marine paleoenvironmental conditions [Coolen and Overmann, 2007]. These C_{org} -rich sedimentary intervals have formed repeatedly in the eastern Mediterranean Sea, in response to precession cycle-triggered maxima in northern Hemisphere solar radiation and intensified African monsoons [de Lange *et al.*, 2008; Rohling and Thunell, 1999]. The oceanic environmental conditions that led to the formation of eastern Mediterranean sapropels have been studied mainly based on isotopic, geochemical and micropaleontological data [e.g., Castradori, 1993; de Lange *et al.*, 2008; Giunta *et al.*, 2003; Principato *et al.*, 2006; Thomson *et al.*, 1999, 2004]. Especially the youngest sapropel S1 (9.8–5.7 ^{14}C kyr B.P. or 10.8–6.1 kyr cal. B.P.), which was deposited during the Early Holocene climate optimum, has been the subject of extensive study [e.g., de Lange *et al.*, 2008; Gennari *et al.*, 2009; Meier *et al.*, 2004; Negri and Giunta, 2001]. An increasingly warmer and wetter climate at the start of the Holocene triggered an increased discharge of freshwater and nutrients from the Nile, which could have resulted in water column stratification and the formation of bottom water anoxia [e.g., de Lange *et al.*, 2008; Emeis *et al.*, 2003; Rohling, 1989], but an enhanced primary production and OM transport also must have played a role in the accumulation of C_{org} -rich sapropels [Calvert, 1983; de Lange and ten Haven, 1983]. Low bottom water oxygen concentrations during S1 deposition are indicated by (1) low amounts or absence of benthic foraminifera [Principato *et al.*, 2006], (2) formation of pyrite with isotopically depleted $\delta^{34}S$ indicative of anoxic sulfidic conditions in sediments and near-bottom water [Passier *et al.*, 1996], (3) a rapid degradation of S1 organic matter when exposed to oxygen [Moodley *et al.*, 2005], and (4) an excellent preservation of delicate organic dinoflagellate cysts [Cheddadi and Rossignol-Strick, 1995; Zonneveld *et al.*, 2001]. A suite of geochemical proxies (e.g., C_{org} content and barite fluxes) recently provided comprehensive evidence that the whole eastern Mediterranean basin was predominantly anoxic below ~1.8 km during the 4 kyr of S1 deposition, whereas more frequent ventilation events resulted in lower C_{org} contents in S1 sediments at shallower depths [de Lange *et al.*, 2008]. In addition, an increase in paleofluxes of the calcifying haptophyte *Florisphaera profunda* coupled with a decrease in the accumulation rate of upper-zone and middle-zone coccolithophorids, suggests an ecological depth separation of the water column, characterized by higher nutrient availability at depth and nutrient-depleted surface waters

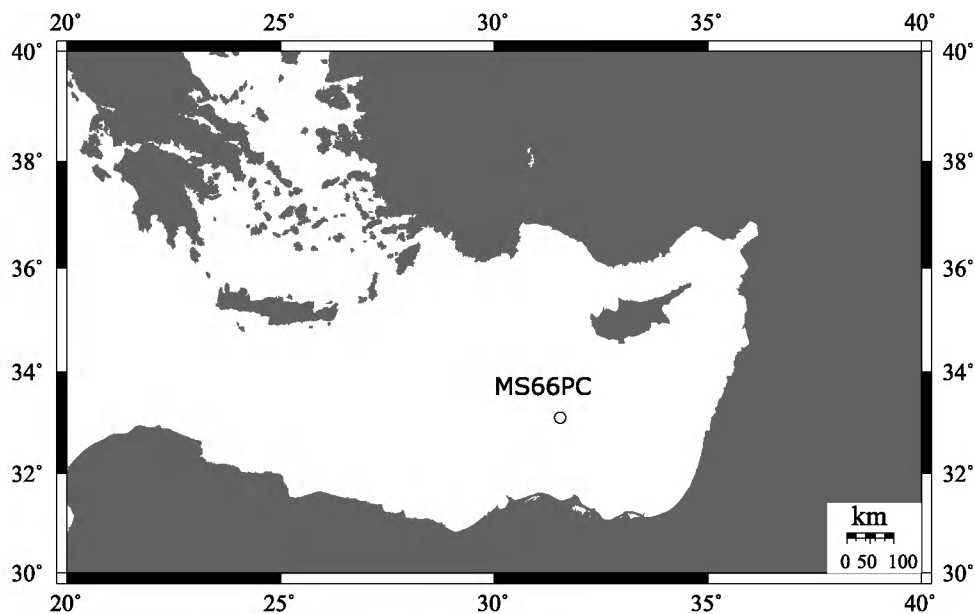


Figure 1. Map of the Mediterranean Sea showing the location of core MS66PC investigated in this study.

during early to mid S1 deposition (9.7–6.5 ^{14}C kyr B.P.) [Principato *et al.*, 2006]. In the present eastern Mediterranean (i.e., nonsapropel times), an extensive remineralization of C_{org} is caused by a well mixed and oxygenated water column and due to the regular formation of new deep and bottom waters in the Adriatic and Aegean Seas [Bethoux, 1993; Casford *et al.*, 2003; Roether and Well, 2001].

[6] In this study we used a comparative multiproxy survey (fossil 18S rDNA, calcareous nannofossils, and lipid biomarkers) to test whether preserved genetic signatures provide an accurate view into haptophyte and dinoflagellate populations during the deposition of the youngest sapropel (S1) and in the C_{org} -depleted marls flanking the S1, and if we could identify important environmental indicator species that did not fossilize and escaped previous microscopic identification. Furthermore, we explored whether fossil DNA stratigraphy as a paleoecological tool can contribute to an increased understanding of the Holocene environmental conditions during deposition of the eastern Mediterranean Sea S1 sapropel.

2. Material and Methods

2.1. Site Description and Sample Collection

[7] During the 2004 MIMES cruise on the R/V *Pelagia*, a piston core (MS66PC) was recovered from near the Nile fan, eastern Mediterranean (location: 33°1.9'N, 31°47.9'E) at a water depth of 1630 m (Figure 1). The 625 cm long core was subsampled onboard and the sediments were placed in sterile 50 ml Greiner tubes and frozen at -40°C immediately. Subsamples were taken at one cm resolution from the S1. Two centimeter intervals at every 10–20 cm were subsampled from the carbonate marls enclosing the sapropel. A total of 18 samples were selected for lipid geochemistry and paleogenetics from the sapropel S1 (~22–65 cm below seafloor), and three subsamples from the enclosing marls above and below the sapropel.

2.2. Geochemical Analyses

[8] Inorganic bulk element analysis was performed on freeze-dried subsamples at the University of Utrecht by Inductively Coupled Plasma–Atomic Emission Spectrometry (ICP–AES) after total digestion [Reitz *et al.*, 2006; Reitz and de Lange, 2006]. Organic carbon and CaCO_3 contents were obtained on a Fisons Instruments CNS NA analyzer using dry combustion at 1030°C [Reitz and de Lange, 2006].

2.3. Molecular Biology

2.3.1. Precautions to Prevent Contamination

[9] Extensive measures were taken to prevent contamination of samples and reagents with foreign DNA as described in previous work [Coolen *et al.*, 2004b, 2009]. At the NIOZ, all DNA extractions and pre-PCR processes were performed in HEPA-filtered and UV-sterilized PCR cabinets inside a PCR product-free lab dedicated to ancient DNA work. All surfaces, pipettes and consumables were decontaminated with RNase-Away™ (Sigma-Aldrich, St. Louis, Missouri, USA) prior to use. Common sense practices such as frequently exchanging disposable vinyl gloves and the use of filter tips during pipetting of reactions also reduce the risk of contamination with foreign nucleic acids. Multiple controls were subjected to the whole extraction (extraction controls; e.c.) and PCR procedure (nontemplate controls; NTC) alongside the samples to monitor possible contamination. No PCR products or any other “high copy number” DNA sources were ever introduced in the cabinets dedicated to ancient DNA analyses, and all downstream applications after PCR were performed in a physically separated laboratory.

2.3.2. DNA Extraction

[10] Total DNA was extracted from 5 to 10 g of wet sediment using the PowerMax™ Soil DNA isolation kit (MoBio laboratories, Carlsbad, California, USA), according to the manufacturers guidelines. The resulting DNA was concentrated using a cold ethanol precipitation, and the

DNA pellet was dissolved in 100 μl of sterile and nucleases-free Tris-EDTA (TE) buffer (pH 8.0) (Ambion). The integrity and yield of DNA in the extracts were checked by agarose gel electrophoresis. Nucleic acid yield was quantified by fluorescence (PicoGreen; MoBiTec, Göttingen, Germany) and found to be between 2 and 15 $\text{ng } \mu\text{l}^{-1}$ within the sapropel layers, and less than 2 $\text{ng } \mu\text{l}^{-1}$ in the enclosing marls.

2.3.3. PCR Conditions

[11] One μl of the purified DNA extracts was subjected to real-time quantitative PCR (qPCR) using primers Pym-429F and Pym-887R [Coolen *et al.*, 2004b] for the selective amplification of a 458 base pair (bp) long region of haptophyte 18S rDNA. A 503 bp long 18S rDNA region of dinoflagellate 18S rDNA was amplified using a general eukaryote forward primer (Euk-1f, [Medlin *et al.*, 1988] and a dinoflagellate-specific reverse primer (Dino_Rev: 5'-ACAAGACATGGATGCCCT-3' [Boere *et al.*, 2009]). The qPCR reactions were run on an Icyler IQ™ real-time PCR detection system (Bio-Rad, Hercules, California, USA) (NIOZ) and a Mastercycler® ep realplex (Eppendorf, Hauppauge, New York) at WHOI, using a SYBR Green I assay. Each 50 μl reaction contained the following reagents and concentrations: 2.5 units PicoMaxx™ High Fidelity PCR System and 1x PicoMaxx buffer (Stratagene, La Jolla, California, USA), 0.25 mM of each dNTPs, 50 μg Bovin Serum Albumin (BSA), 1 mM MgCl_2 , 1x SYBR® Green I, 10 nM Fluorescein (only with the iCycler), and 0.2 μM of each of the primers, and DNA-free PCR water (Sigma-Aldrich, St. Louis, Missouri, USA) was added to 50 μl . All PCR programs contained an initial denaturing step at 96°C for 4 min, followed by a number of amplification cycles outlined below comprising a denaturing step (94°C, 40 s), an annealing step ($T_a = 62^\circ\text{C}$ for haptophytes and $T_a = 63.5^\circ\text{C}$ for dinoflagellates, 40 s), an elongation step (72°C, 60 s) and a photo step (80°C, 20 s). A final elongation step (72°C, 10 min) was added for the quantification reaction. A 10-fold dilution series of reactions containing from 10^0 to 10^7 copies of full-length 18S rDNA of *Emiliania huxleyi* was used as a standard to quantify the absolute number of haptophyte 18S rDNA copies in our samples. To quantify the amount of preserved sedimentary dinoflagellates rDNA, full-length rDNA of *Scrippsiella sp.* was used. The qPCR data was expressed as number of (partial) gene copies per gram of total organic carbon (copies $\text{g}^{-1} \text{C}_{\text{org}}$) in order to compensate for variable organic content between the analyzed sediment intervals.

[12] Quality and length of the produced PCR amplicons was checked by a melting curve analysis and by standard agarose gel electrophoresis followed by ethidium bromide staining. In the melting curve analysis, fluorescence in each sample was measured during a stepwise increase of the temperature from 60°C to 96°C in 0.5°C temperature increments.

2.3.4. Denaturing Gradient Gel Electrophoresis (DGGE)

[13] One μl of the PCR-amplified samples and negative controls was subjected to a second round of PCR using 12 cycles to generate template DNA for subsequent DGGE analysis. The 20 μl reaction mixtures contained fresh PCR reagents, with the same forward primer but a modified reverse primer. A GC clamp, that is, a 40 base pair long GC-rich tag was attached to this reverse primer. The addi-

tion of a GC clamp prevents complete dissociation of the two strands and loss of amplicons during DGGE analysis [Muyzer *et al.*, 1993]. The resulting reamplified PCR products were checked and quantified on agarose gel, and ~100 ng per sample was brought on a DGGE gel which contained a 20–60% gradient of denaturing chemicals (urea and formamide). After running for 5 h at 200 V (12.5 V cm^{-1}), the gel was stained for ~20 min with SYBR® Gold (Invitrogen, Carlsbad, California, USA) and visualized using a Dark Reader (Clare Chemicals Research, Dolores, Colorado, USA). Subsequently, 39 bands of dinoflagellate 18S rDNA and 21 bands of haptophyte 18S rDNA were excised and sequenced, both including a number of bands from similar position in the gel in order to check if they indeed represent the same phylotypes (e.g., following Coolen *et al.* [2006a]). All PCR-amplified controls for contamination remained negative, also after the second round of PCR.

2.3.5. Sequencing and Phylogenetic Analyses

[14] Sequencing of the excised DGGE bands was done by Macrogen Inc. (Seoul, South Korea). Similar sequences were identified by a BLAST search on the NCBI homepage (www.ncbi.nlm.nih.gov). The sequences were then imported into the ARB package [Ludwig *et al.*, 2004] and were aligned using the FAST aligner utility with the approximately 50,000 prealigned eukaryote sequences in the SILVA database (release 93 [Pruesse *et al.*, 2007]). The alignment was subsequently checked and refined manually. Similar bands were grouped into operational taxonomic units (phylotypes) using a 98% sequence similarity cutoff value using the program DOTUR [Schloss and Handelsman, 2005]. The 15 unique phylotypes (9 dinoflagellates and 6 haptophytes) recovered in this study are deposited in the NCBI database under accession numbers FJ717393–FJ717407.

[15] These consensus sequences were exported from ARB, and along with selected similar sequences and sequences of morphologically preserved species, analyzed in MEGA4 [Tamura *et al.*, 2007]. Whenever available in NCBI, we included sequences of haptophyte species that were present in the calcareous nannofossil assemblage. These species included: *Emiliania huxleyi*, *Gephyrocapsa oceanica*, *Syracosphaera pulchra*, *Coronosphaera mediterranea*, *Scyphosphaera apsteinii*, *Calcidiscus leptopus* and *Umbilicosphaera sibogae*. Included available sequences through NCBI that were related, but not identical, to dinoflagellate species of previously described dinocysts in eastern Mediterranean Holocene S1 sediments [Zonneveld *et al.*, 2001] involve dinoflagellates of the genera *Scrippsiella* and *Prorocentrum*. A Neighbor joining analysis was run, using the Jukes-Cantor model and assuming uniform rates among sites. A consensus tree which shows only splits with bootstrap support >50% (1000 bootstrap replicates) was finally generated.

2.4. Lipid Geochemistry

[16] Wet sediments (~5 g) were freeze-dried and subsequently ultrasonically extracted 5 times with dichloromethane/methanol (DCM/MeOH; 2:1, v/v). The solvent was removed by rotary evaporation under vacuum. The extracts were methylated with diazomethane and separated by column chromatography on Al_2O_3 into apolar (containing alkenones) and polar fraction using DCM and DCM/MeOH (1:1, v/v)

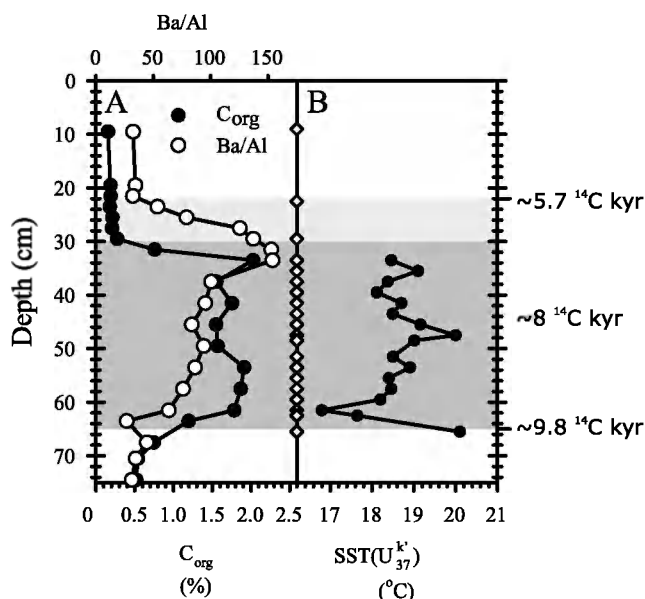


Figure 2. Sedimentary profiles of core MS66PC. (a) Organic carbon (C_{org}) content in core MS66PC as percentage of the total sediment weight (solid circles) and the Ba/Al ratio (open circles). (b) Sea surface temperature (SST) estimated for the sapropel S1 based on the alkenone-based U_{37}^k paleothermometer. The approximate interval of the sapropel S1 is shown as gray shaded area, and the part of S1 that was reoxidized after reventilation of the bottom waters is shown in lighter gray. The ^{14}C ages of the onset and termination of the original sapropel are shown on the right-hand side [de Lange *et al.*, 2008]. Depths that were used in the paleogenetic analysis are marked with a diamond on the middle y axis.

as the eluent, respectively. To the apolar fractions an internal standard (6,6-d2-3-methyl-eicosane) was added and they were analyzed by gas chromatography (GC) and gas chromatography-mass spectrometry (GC/MS). The same internal standard (6,6-d2-3-methyl-eicosane) was added to half of the polar fraction and this total lipid fraction was subsequently silylated with bis(trimethyl)trifluoroacetamide (BSTFA) at 60°C for 20 min and analyzed by GC and GC/MS.

[17] To quantify the biomarker concentrations, GC analyses were performed using a Hewlett-Packard 5890 instrument equipped with a flame ionization detector (FID) and an on-column injector. A fused silica capillary column (25 m \times 0.32 mm i.d.) coated with CP-Sil 5 (film thickness 0.12 μ m) was used with helium as carrier gas. The oven was programmed at a starting (injection) temperature of 70°C, and programmed to 130°C at 20°C min^{-1} and then to 320°C at 4°C min^{-1} , at which it stayed for 10 min.

[18] The different fractions were analyzed by GC/MS using a Finnigan Trace GC Ultra coupled to a Finnigan Trace DSQ mass spectrometer. GC conditions and column were as described above. The column was directly inserted into the electron impact ion source of the DSQ quadrupole mass spectrometer, scanning a mass range of m/z 50–800 at 3 scans per second and an ionization energy of 70 eV.

2.5. Microscopical Analysis of Calcareous Nannofossils

[19] Five samples were selected for micropaleontological analyses of calcareous nannofossils (sample depths 36.5, 40.5, 44.5, 52.5 and 58.5 \pm 0.5 cm). Samples were prepared following the standard smear slide techniques and analyzed with a polarized light microscope (PLM) at 1250X. Semi-quantitative analyses of nannofossil species occurrence and abundance were performed for each slide through a count of approximately 300 specimens. For the identification of rare species, a fixed area of 150 fields of view was examined.

3. Results

3.1. Organic Carbon (C_{org}), Ba/Al

[20] C_{org} values were low in sediments between 75 and 68 cm (\sim 0.5 wt%) and in the upper 30 cm (\sim 0.2 wt%). Elevated amounts of C_{org} ranging between 1.5 and 2% were measured between 63 and 32 cm (Figure 2a). The Ba/Al ratio gradually increased with decreasing sediment depth and reached a maximum value of \sim 150 at 30 cm (Figure 2a). This ratio was also elevated in the C_{org} -depleted sediments between 30 and 22 cm, indicative that this part of the core was reoxidized after the return of a well-ventilated water column [cf. de Lange *et al.*, 2008; Thomson *et al.*, 1999], and that the S1 in our core is located at depths between 65 and 22 cm.

3.2. Quantitative Analysis of Preserved Dinoflagellate and Haptophyte 18S rRNA Genes

[21] Throughout S1, the amount of preserved 500 bp long dinoflagellate 18S rDNA fragments exceeds that of similar-sized haptophyte 18S rDNA by one order of magnitude (Figures 3 and 4). The dinoflagellate 18S rDNA content was highest at 53 cm (2.2×10^7 copies $g^{-1} C_{org}$) with 2 to 10 times lower concentrations in the deeper and shallower intervals of S1 (Figure 3). Preserved haptophyte 18S rDNA (10^5 – 10^6 copies $g^{-1} C_{org}$) was often near the detection limit (\sim 10^5 copies $g^{-1} C_{org}$), especially between 42 and 30 cm, which hampers the reproducibility of the quantitative results and leads to relatively large error bars (Figure 4). Both dinoflagellate and haptophyte 18S rRNA gene sequences were below the detection limit in the reoxidized part of S1 (30–22 cm) as well as in the C_{org} -poor marls flanking sapropel S1.

3.3. Dinoflagellate Communities During the Development of Sapropel S1

[22] We were unable to amplify 500 bp long dinoflagellate 18S rDNA fragments from the total DNA pool extracted from the oxidized part of the S1 between 30 and 22 cm (Figures 2 and 3). However, the development of the dinoflagellate paleocommunity during the deposition of the C_{org} -rich part of sapropel S1 shows three distinct intervals in the DGGE (intervals D-I through D-III; Figure 3). A total of 39 dinoflagellate bands were excised from the gel of which 36 bands were successfully sequenced. The sequenced bands were aligned and grouped into phylotypes using a 98% sequences similarity value. The nine resulting unique phylotypes (A-I) and selected relevant sequences available through NCBI with highest similarities to phylotypes A-I were used in a Neighbor Joining phylogenetic analysis

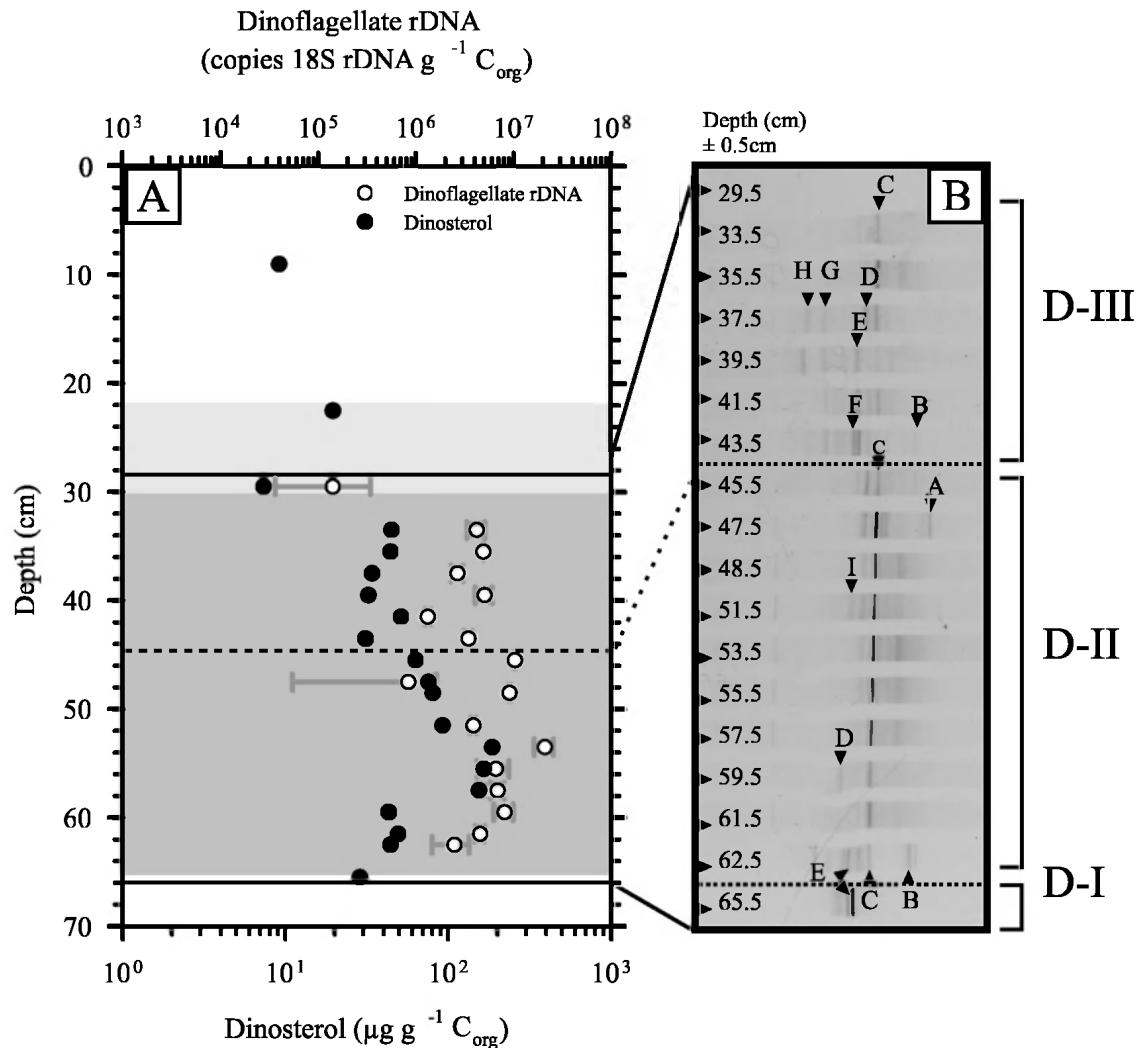


Figure 3. (a) Preserved dinoflagellate DNA, expressed as number of copies of the partial 18S rDNA, normalized per gram of total organic carbon (copies $\text{g}^{-1} \text{C}_{\text{org}}$; open circles) and concentration of dinoflagellate biomarker dinosterol ($\mu\text{g g}^{-1} \text{C}_{\text{org}}$; solid circles). (b) DGGE with fossil DNA preserved in the Holocene sapropel S1 showing changes in the dinoflagellate community. Partial 18S rDNA was amplified using a dinoflagellate-specific primer set (Euk-1A and Dino-rev) and separated using DGGE. A total of 39 bands were excised and sequenced; sequences were clustered (using a 98% cutoff value) into nine unique phylotypes (dinoflagellate phylotype A-I). Depth values are the average of 1 cm thick sediment slices (± 0.5 cm).

(Figure 5). Interval D1 (65 cm) was the only C_{org} -depleted sediment layer that, despite the extremely low dinoflagellate DNA content (Figure 3a), revealed a single phylotype (phylotype E; FJ717397; Figure 3b). The amount of preserved dinoflagellate DNA was much higher in the C_{org} -rich early to mid S1 (varying between 10^6 and 10^7 copies $\text{g}^{-1} \text{C}_{\text{org}}$; Interval D-II, 62–45 cm), but despite more DNA template for PCR, the dinoflagellate diversity (phylotypes C, D, and I) was not much higher than in the C_{org} -depleted marl sample directly below S1. Within Interval D-II, phylotype C (FJ717395) represented the most abundant species with lower contributions of phylotypes D (FJ717396) and I (FJ717401). Sequences with the highest similarities with phylotypes C (BS-Euk-DGGE-08; 100%), and phylotype D (BS-Euk-DGGE-10; 98%, Figure 5) were recovered from anoxic and sulfidic Holocene Black Sea sediments [Coolen *et al.*, 2006a].

The highest diversity of dinoflagellates (phylotypes B-E and F-H), was found in interval D-III (45–33 cm). Within this youngest C_{org} -rich interval of S1, phylotype C became less abundant and was below detection limit in some of the analyzed sediment layers. The majority of the phylotypes that were only detected in interval D-III were related to sequences found in normal coastal or oceanic settings and have not been identified from stratified anoxic settings (Figures 3 and 5). For example, phylotypes A (FJ717393) and B (FJ717394) have no known close relatives, but are most closely related to species derived from the water column at 500 m depth in the Sargasso Sea (eukaryote clone SSRPB60; [Not *et al.*, 2007]) in this analysis. The most closely related sequences of phylotypes F (99%) were an uncultured clone isolated from surface seawater (clone BTQB20030806.0094) and coastal *Scrippsiella* spp. (Figure 5).

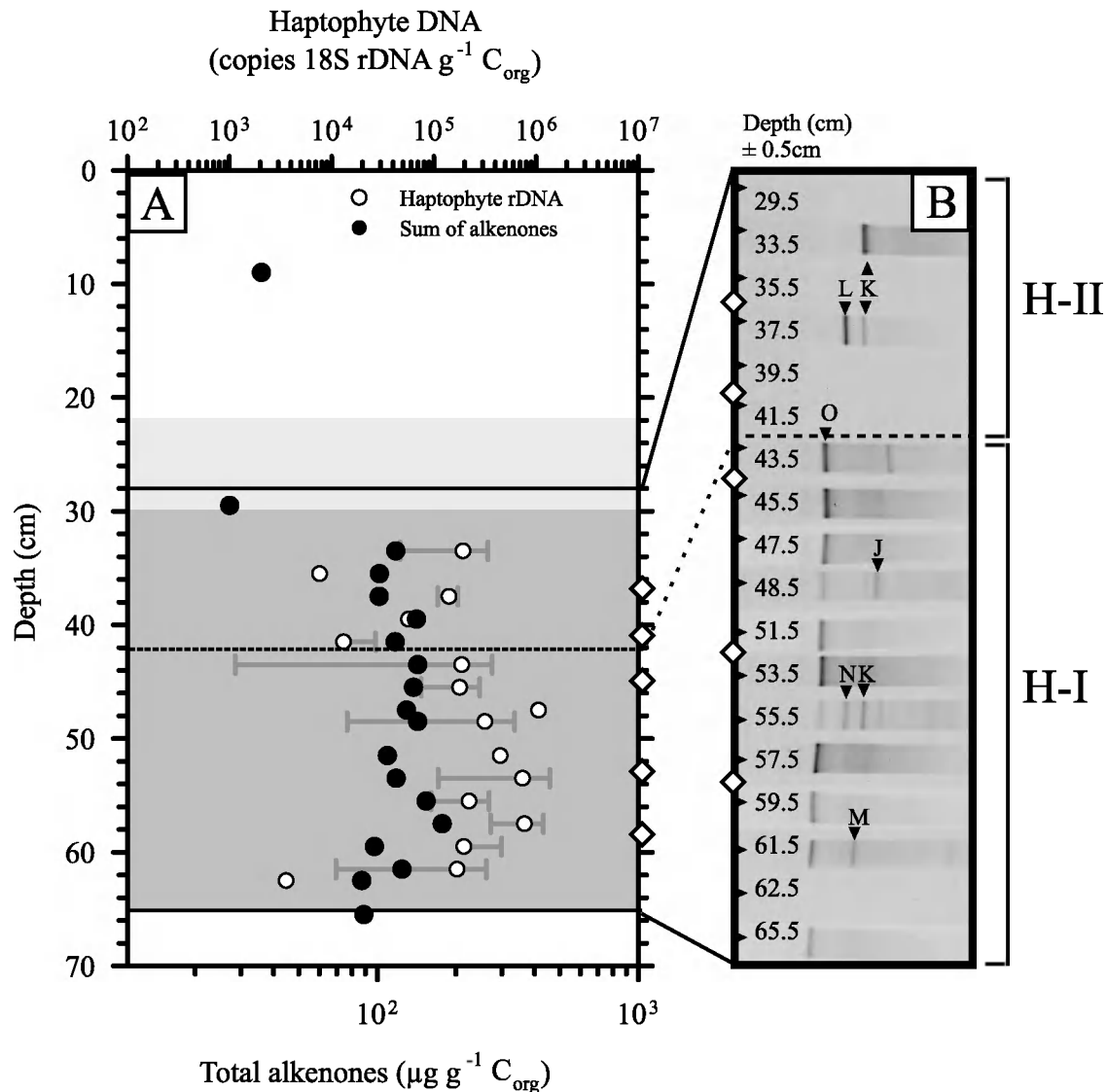


Figure 4. (a) Preserved haptophyte DNA, expressed as the number of copies of partial 18S rDNA, normalized per gram C_{org} (copies g⁻¹ C_{org}; open circles) and the sum of dominant alkenones C_{37:2}, C_{37:3} and C_{38:3} (μg g⁻¹ C_{org}; solid circles). The five samples that were analyzed for nanofossil association are marked on the right axis with open diamonds. (b) DGGE with preserved partial 18S rDNA in the Holocene sapropel S1 showing changes in the haptophyte paleocommunity. Partial 18S rDNA was amplified using haptophyte-specific primers Pym-429F and Pym-887R and separated using DGGE. A total of 17 bands were excised and sequenced, and sequences were clustered (using a 98% cutoff value) into six unique phylotypes (haptophytes phylotypes J-O). Depths are given as the average of 1 cm thick sediment slices (±0.5 cm).

3.4. Haptophyte Communities During the Development of Sapropel S1

[23] Similar-sized partial haptophyte 18S rRNA gene fragments were also only recovered from C_{org}-depleted marl just below the S1 as well as the C_{org}-rich part of the S1

(Figure 4). Seventeen out of twenty-one excised haptophyte DGGE bands could successfully be sequenced and were grouped into 6 phylotypes based on a 98% sequence similarity value (haptophyte phylotypes J-O, Figures 4 and 6). Haptophyte DNA was close to the detection limit in the

Figure 5. Consensus tree with partial 18S rDNA sequences recovered from the Holocene eastern Mediterranean sediment record (marked in bold) with 18S rDNA sequences of similar dinoflagellate sequences available through the NCBI database for comparison. The bootstrap consensus tree was built using the Neighbor Joining method (JC model, uniform substitution rates) in the program MEGA4. The percentage of replicate trees in which the associated taxa clustered together in the bootstrap test (1000 replicates) is shown next to the branches. Branches corresponding to partitions reproduced in less than 50% bootstrap replicates are collapsed.

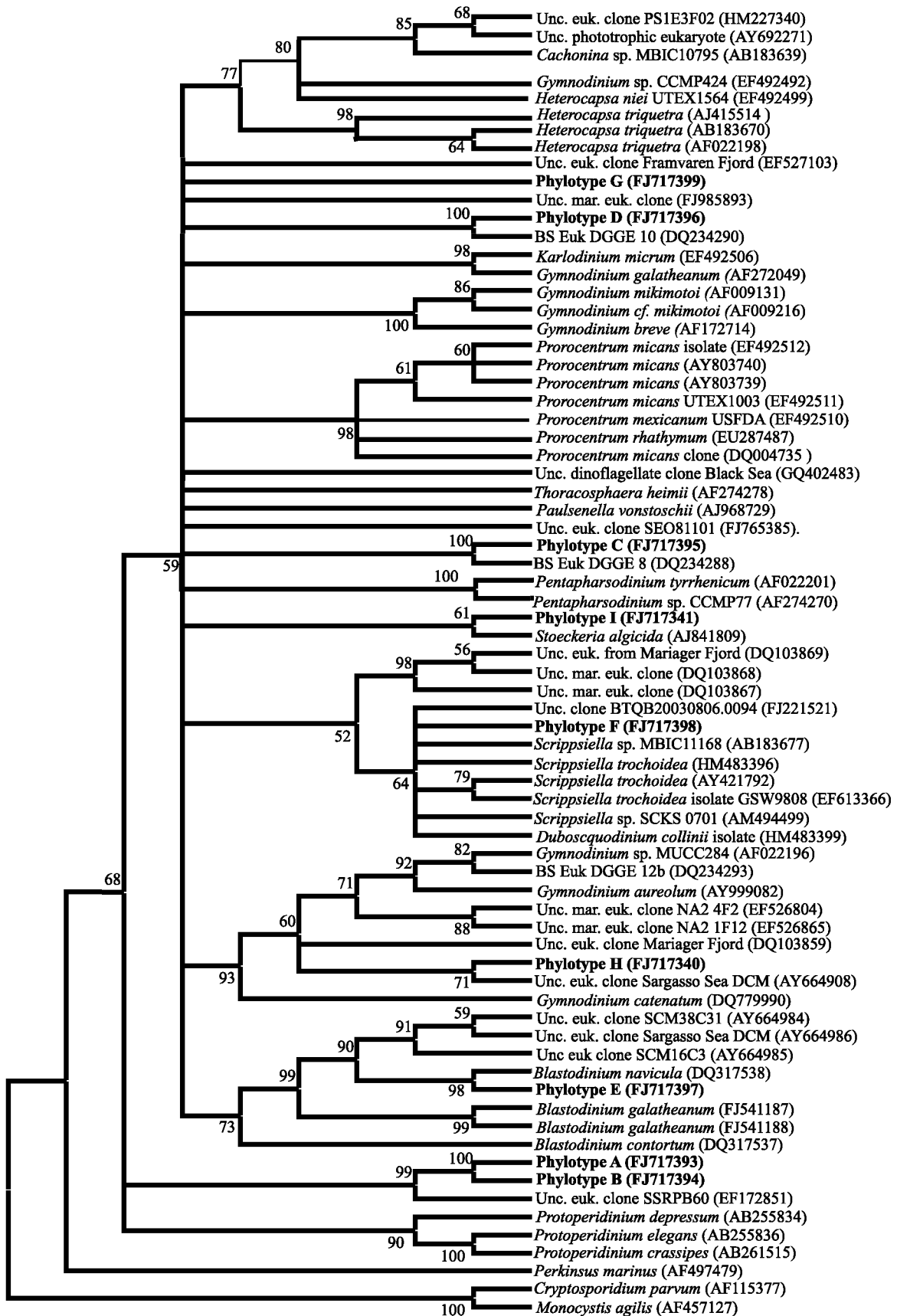


Figure 5

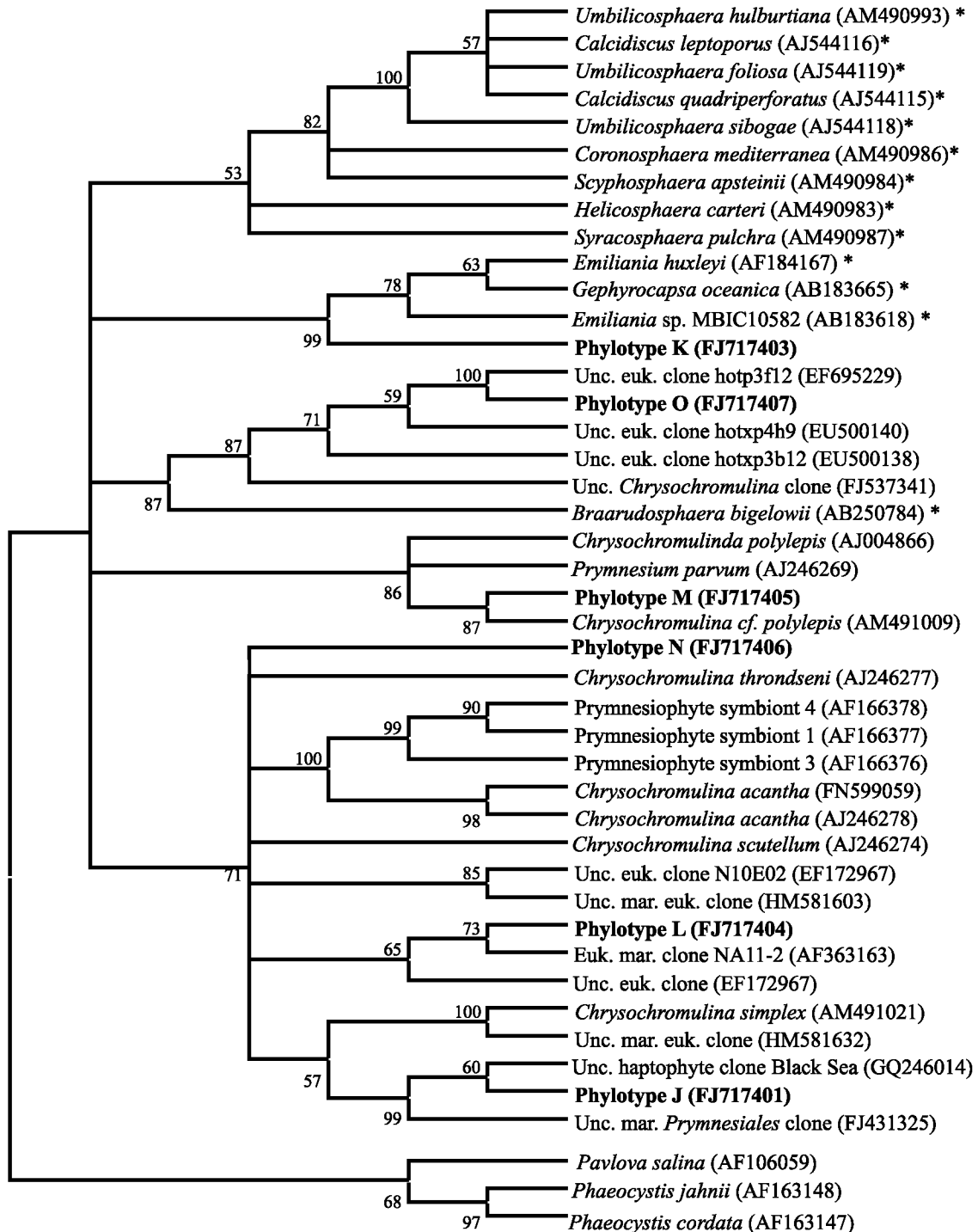


Figure 6. Consensus tree with partial 18S rDNA sequences recovered from the Holocene eastern Mediterranean sediment record (marked in bold) and 18S rDNA sequences of haptophyte species that were found as calcareous nannofossils in the same sediment record (marked with asterisks) as well as similar sequences available through the NCBI database for comparison. The bootstrap consensus tree was built using the Neighbor Joining method (JC model, uniform substitution rates) in the program MEGA4. The percentage of replicate trees in which the associated taxa clustered together in the bootstrap test (1000 replicates) is shown next to the branches. Branches corresponding to partitions reproduced in less than 50% bootstrap replicates are collapsed.

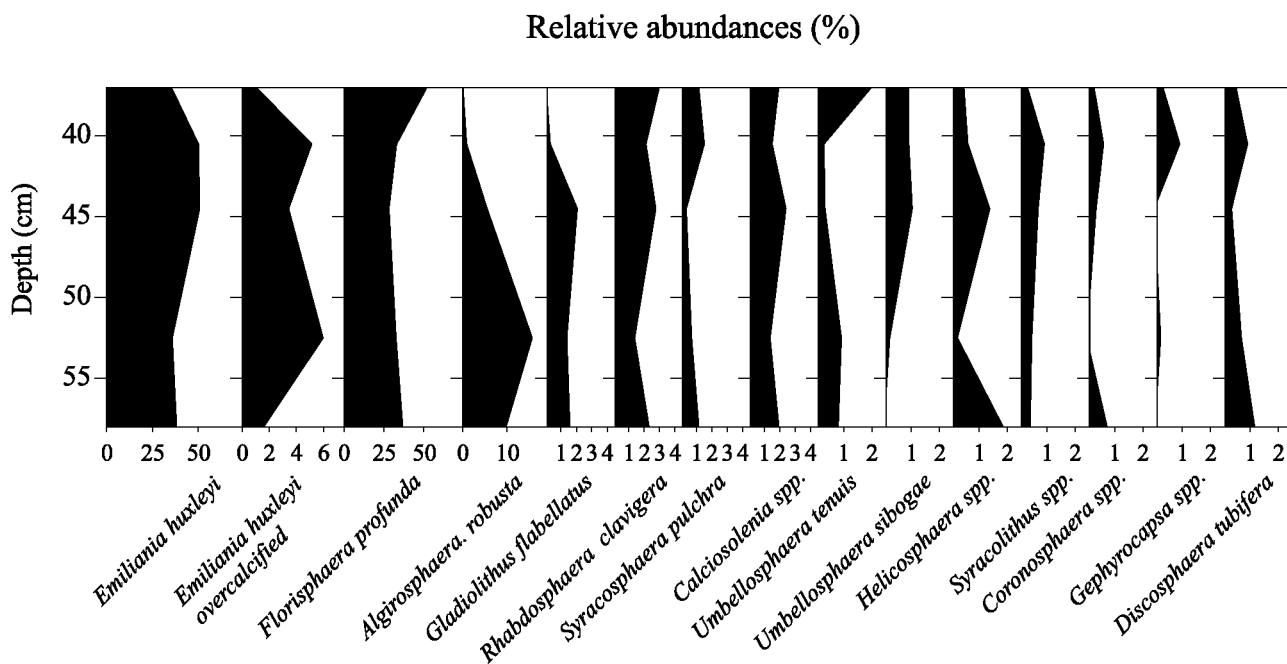


Figure 7. Relative abundances (%) of the most dominant calcareous nannoplanktonic species.

deepest analyzed sample from the C_{org} -depleted marl just below the S1. Whereas the fossil dinoflagellate DNA survey recorded a unique community in this “pre-S1 marl,” the haptophyte community in this layer and in the lower part of the S1 was identical. We, therefore, identified two intervals with unique haptophyte populations as opposed to the three intervals with unique dinoflagellate populations. According to the fossil DNA survey, a major shift in the haptophyte community occurred at 43 cm in our sediment record (Figure 4b), which coincided with the observed major shift in the dinoflagellate population (Figure 3b). Haptophyte phylotype O (FJ717407), which cooccurred with dinoflagellate phylotype C between 65 and 43 cm (Interval H-I), showed greatest sequence similarity (99.5%) with uncultivated haptophytes that, according to RNA stable isotopic probing experiments, were capable of mixotrophic growth as predators on picocyanobacteria [Frias-Lopez et al., 2009]. Phylotype O was below detection limit in interval H-II (<43 cm).

[24] Despite several attempts, haptophyte sequences of the correct fragment length (458 bp) were only recovered from interval H-II at depths between 37.5 ± 0.5 cm and 33.5 ± 0.5 cm: Phylotype K (FJ717403) occurred in both intervals and showed 98% sequence similarity with the alkenone-producing coccolithophorids *Emiliana huxleyi* and *Gephyrocapsa oceanica*. Phylotype L was only recovered from interval H-II and showed 98% sequence similarity to a clone recovered from the North Atlantic [Diez et al., 2001].

3.5. Fossil Lipid Biomarkers Diagnostic for Dinoflagellates and Haptophytes

[25] Dinosterol (4 α ,23,24-trimethyl-5 α -cholest-22E-en-3 β -ol), the lipid biomarker of many but not all dinoflagellates [Volkman et al., 1998], was identified in all analyzed layers of sapropel S1 (Figure 2). The average concentration was ~ 50 – $90 \mu\text{g g}^{-1} C_{org}$ throughout sapropel S1, except for an

interval close to the basal part of the sapropel (~ 52 and 58 cm) where dinosterol reached maximum concentrations of up to $\sim 200 \mu\text{g g}^{-1} C_{org}$. Dinosterol concentrations were significantly lower (< 10 – $20 \mu\text{g g}^{-1} C_{org}$) in the organic carbon-lean enclosing marls and in the reoxidized part of S1.

[26] The concentration of fossil haptophyte-derived long-chain alkenones was fairly constant throughout sapropel S1 (100 – $150 \mu\text{g g}^{-1} C_{org}$; Figure 4). The predominant alkenones were the two- and three-times unsaturated C_{37} methyl ketones used in U_{37}^k paleothermometry ($C_{37:2}$ and $C_{37:3}$ methyl ketones (mK); together comprising $\sim 60\%$ of the total alkenone content). C_{38} alkenones represented the remaining $\sim 40\%$ of the total alkenone content. As for dinosterol, alkenones were less abundant (0 – $20 \mu\text{g g}^{-1} C_{org}$) in the C_{org} -poor marls and in the reoxidized part of S1.

[27] U_{37}^k -based sea surface temperature (SST) estimates gradually increased from 17 to 19°C between early and mid sapropel deposition (63 – 48 cm depth; Figure 2b) and a peak in SST (20°C) was observed at ~ 46 cm. The SST then dropped slightly again and remained relatively constant at $\sim 18^\circ\text{C}$ above 44 cm. No reliable SST estimate could be obtained from the C_{org} -poor marls below and above sapropel S1 since alkenone concentrations were generally low and $C_{37:3}$ was below the detection limit.

3.6. Identification of Calcareous Haptophyte Nannofossils in Sapropel S1

[28] In the youngest of the analyzed sapropel S1 sample (36.5 cm), the calcareous nannofossil assemblage was dominated by *Emiliana huxleyi* (55%), followed by *F. profunda* (33%) with a contribution of minor species (Figure 7). The heavily calcified morphotype of *E. huxleyi* (as described by Crudele et al. [2004]) (Figure 8) was present in all samples but most abundant at 52.5 cm and at 36.5 cm (Figure 7). Within the older part of the sapropel, *F. profunda* ranges from 28 to 37% , but becomes more abundant than *E. huxleyi* at

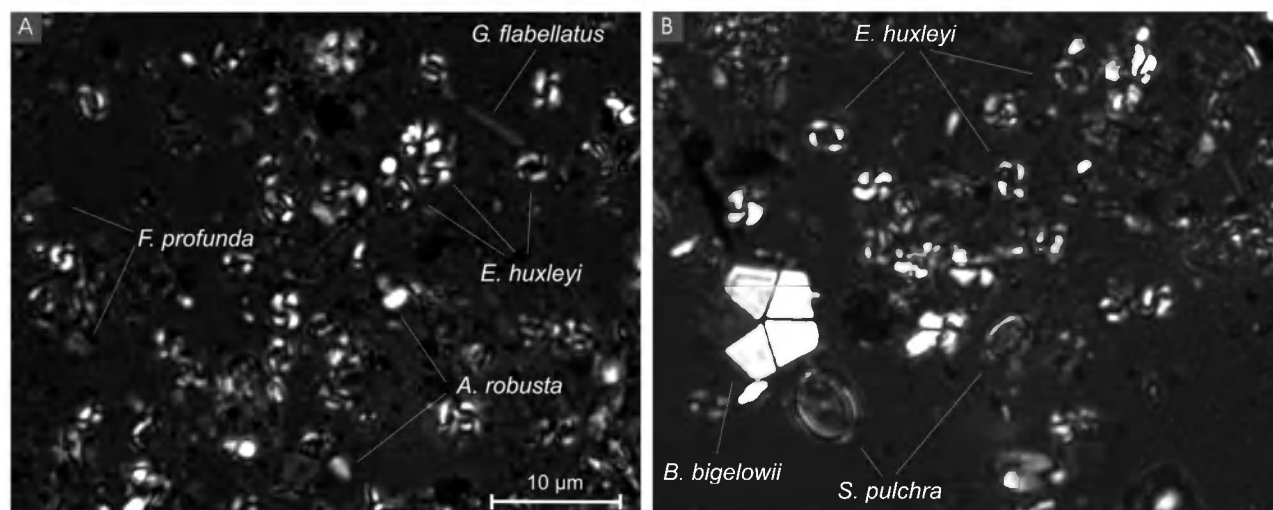


Figure 8. (a) The typical nannofossil association in the samples from the lower part of the S1 sapropel. (b) The isolated occurrence of the large morphotype of *Braarudosphaera bigelowii* within the *Emiliantia huxleyi*-dominated nannofossil association.

36.5 cm. *A. robusta* is another locally important species, which is abundant in the older part of the sapropel (5 to 16%) but absent in the youngest analyzed interval at 36.5 cm.

[29] Overall, minor species include: *Rhabdosphaera clavigera*, *Calciosolenia brasiliensis*, *Syracosphaera pulchra*, *Umbellosphaera tenuis*, *Syracolithus spp.*, *Helicosphaera spp.*, *Umbilicosphaera sibogae*, *Coronosphaera spp.*, *Discosphaera tubifera* and rare *Calcidiscus leptoporus*, *Pontosphaera spp.*, and *Scyphosphaera apsteinii*. Isolated occurrences of medium and large morphotypes of the pentoliths of *Braarudosphaera bigelowii* were detected in sediments up to 47.5 cm (Figure 8), but these pentoliths were not found above 47.5 cm.

4. Discussion

[30] Our parallel stratigraphic analysis of dinoflagellate (fossil DNA and dinosterol) and haptophyte (fossil DNA, long-chain alkenone biomarkers, and nannofossils) markers enabled us to cross validate the presence of each paleoecological proxy prior, during, and after eastern Mediterranean S1 deposition. We will first discuss the suitability of fossil DNA as a paleoecology proxy for dinoflagellates and haptophytes followed by a discussion of paleoenvironmental information inferred from the fossil DNA signatures and how well this correlates with existing views on the environmental conditions in the eastern Mediterranean Sea during the Holocene.

4.1. Validating Fossil DNA as a Proxy for Holocene Mediterranean Dinoflagellates

[31] Whereas all earlier mentioned fossil DNA studies focused on reconstructing the ancient plankton ecology in permanently stratified, anoxic and sulfidic lake and marine settings, this is the first attempt of using paleogenetics to study plankton DNA that was deposited in the presence of bottom water anoxia (early S1) [e.g., *de Lange et al.*, 2008; *Principato et al.*, 2006] as well as in the presence of a well-mixed water column and fully oxygenated bottom waters

and surface sediments (i.e., during deposition of C_{org} -depleted sediments) [*Bethoux*, 1993; *Casford et al.*, 2003; *Roether and Well*, 2001].

[32] C_{org} -depleted sediments flanking the S1 as well as the oxidized upper part of the S1 contained low concentrations of dinosterol, but only the oxidized marl that was deposited just before the onset of the formation of the C_{org} -rich part of the S1 (65.5 ± 0.5 cm; interval D-I), still contained traces of detectable 500 bp long dinoflagellate 18S rDNA. Most likely, a fraction of the fossil DNA in this layer survived degradation due to a much shorter postdepositional exposure to oxidative damage [*Lindahl*, 1993] as opposed to the DNA in all other analyzed C_{org} -depleted layers.

[33] A single dinoflagellate (phylogroup E) with up to 99% sequence similarity to 18S rRNA gene sequences of known marine copepod parasites of the genus *Blastodinium* [*Skovgaard*, 2005] was detected in interval D-I. This phylogroup branches closely enough with *Blastodinium* sequences to assume that it represents a past copepod parasite of this genus [*Skovgaard et al.*, 2007]. The detection of phylogroup E is of paleoecological interest since it shows the potential of using paleogenetics to identify past parasite/host interactions. On the other hand, the presence of phylogroup E does not provide paleoenvironmental information.

[34] PCR/DGGE selects for the most abundant phylogroups present [*Coolen et al.*, 2007], but the actual detected dinoflagellate diversity in interval D-I must be underestimated due to the low number of preserved 18S rDNA copies that were available for PCR amplification. A parallel analysis of preserved calcareous and organic-walled dinoflagellates cysts of this core was not performed, but up to 5 million calcareous dinoflagellate cysts per gram sediment, with *Thoracosphaera heimii* and *Sphaerodindella tuberosa* variants as the most abundant species, were reported in a comparable “pre-S1 layer” [*Zonneveld et al.*, 2001]. Organic-walled cysts were several orders of magnitude less in abundance [*Zonneveld et al.*, 2001]. Clearly, the paleogenetics approach did not detect any of those species in our pre-S1

interval. This could either be due to the degradation of DNA to less than 500 bp long fragments, even inside intact cysts, or that our extraction method failed to lyse DNA from the cysts. The former explanation is more likely since the stringent DNA extraction method includes vigorous chemical and mechanical (i.e., bead beating) cell disruption steps, and *Blastodinium* related species represented by phylotype E is known to form dinospores (free living stage) or to occur as a theca-covered multicellular form (parasitic stage) [Skovgaard *et al.*, 2007]. Moreover, we successfully used this DNA extraction approach in prior studies and were able to extract large amounts of DNA from, for example, *Chaetoceros* diatom cysts [Coolen *et al.*, 2007]. Assuming that phylotype E was derived from the parasitic theca-covered multicellular form of *Blastodinium*, this life cycle has little resemblance to typical dinoflagellate morphologies [Skovgaard *et al.*, 2007], which then could have been a reason why this species escaped prior microscopical identification from the eastern Mediterranean Holocene sediment record. A preferred sequestration of DNA of the parasitic multicellular and difficult to determine life cycle of *Blastodinium* is likely due to a higher DNA content in a multicellular stage as opposed to single celled free living dinospores, a protective theca covering, and an effective transport to the sediment upon death of a large and fast sinking host.

[35] The highest dinosterol concentrations and up to 2×10^7 copies $\text{g}^{-1} \text{C}_{\text{org}}$ of predominantly phylotype C were found in interval D-II, but the genetic and lipid biomarker depth profiles were not identical (Figure 3). It has recently been reported that shifts in dinoflagellate communities from dinosterol producing species to species that do not produce dinosterol may lead to misinterpretation of fossil dinosterol profiles [Boere *et al.*, 2009]. On the other hand, it is possible that some of the species found in the fossil cyst assemblage of comparable Holocene eastern Mediterranean sediments [Zonneveld *et al.*, 2001] were sources of dinosterol, but were missed with our paleogenetics approach. For example, *Scrippsiella regalis* represented one of the less abundant cysts [Zonneveld *et al.*, 2001], and *Scrippsiella* species were proven to be sources of dinosterol [Harvey *et al.*, 1988; Mansour *et al.*, 2003]. It is thus possible that differences between the amounts of dinosterol versus 18S rDNA (Figure 3) were caused by a preferential degradation of DNA from alternate sources of dinosterol. In addition, it should be mentioned that the number of genomic 18S rRNA gene copies varies in eukaryotes, especially among dinoflagellates [Godhe *et al.*, 2008; LaJeunesse *et al.*, 2005]. However, the dinoflagellate species composition dramatically changed between intervals D-II and D-III whereas the number of rDNA copies only changed by less than a factor of five between sediment horizons. Therefore, the variation in genomic and cellular 18S rDNA copy numbers between species must have been limited. One last possibility for the observed discrepancies is that morphologically intact dinocysts, or those species that produced dinosterol, only represent a minor fraction of the total sedimentary dinoflagellate biomass. It has namely recently been shown that extracellular DNA from degraded cells is much more abundant than intracellular DNA from intact cells in a variety of marine sediments [e.g., Corinaldesi *et al.*, 2008]. PCR might have selected for the most abundant sequences that are present in the extracellular DNA pool. Despite these discrepancies, the

observed fossil DNA-inferred dinoflagellate species succession through time does nevertheless record environmental changes as discussed later.

4.2. Validating Fossil DNA as a Proxy for Holocene Mediterranean Haptophytes

[36] All analyzed sediments including the C_{org} -poor marl layers and the oxidized upper part of S1 contained long-chain alkenones indicative of the preservation of ancient haptophyte biomass in all sediment horizons (Figure 4). However, PCR-amplifiable 460 bp long haptophyte 18S rDNA could only be recovered from the C_{org} -rich part of the S1 and from the C_{org} -poor layer just below the S1. All alkenone producing haptophytes cluster within the order *Isochrysidales* and comprise the calcifying *Emiliania huxleyi* and its closely related ancestor *Gephyrocapsa oceanica*, both with identical full-length 18S rRNA gene sequences, as well as nonfossilizing and phylogenetically more diverse species (i.e., *Isochrysis* spp. and *Chrysolita lamellosa*) [Marlowe *et al.*, 1984; Rontani *et al.*, 2004; Versteegh *et al.*, 2001; Volkman *et al.*, 1995]. None of the detected haptophyte sequences were related to the noncalcifying alkenone producing haptophytes, and phylotype K was not identical (98% sequence similarity) to the closely related calcifying alkenone producers *E. huxleyi* and *G. oceanica* (Figures 4 and 6). According to the nannofossil data set, *E. huxleyi* comprised on average 50–60% of the coccolith assemblage in all five selected sediment horizons spanning early, mid, and late sapropel deposition (Figure 7), and other studies have also shown that the calcareous nannofossil association preserved in sapropel S1 sediments is usually dominated by *E. huxleyi* [Castradori, 1993; Negri and Giunta, 2001; Principato *et al.*, 2003; Thomson *et al.*, 2004]. The failure to identify a phylotype with identical sequence to *E. huxleyi* 18S rDNA is surprising since genetic markers of *E. huxleyi* including 18S rDNA was found to be well preserved in anoxic Holocene coccolith-bearing sediments of the Black Sea, but also in the underlying organic-rich Black Sea sapropel where coccoliths were most likely absent as a result of postdepositional dissolution [Coolen *et al.*, 2006a, 2009]. These differences in the level of preservation of DNA versus coccoliths of *E. huxleyi* could reflect differences in (post)depositional environmental conditions between the Mediterranean Sea during S1 deposition and the Black Sea. Periodic ventilation to a depth of 1630 m at our coring site [Casford *et al.*, 2003; de Lange *et al.*, 2008] could have resulted in a lower level of DNA preservation as opposed to similar-aged fossil algal DNA in the Holocene Black Sea sediments, which were continuously anoxic and exposed to sulfidic conditions.

[37] Our fossil DNA survey did not identify any of the additional calcareous haptophyte species that were represented in the nannofossil assemblage. For instance, we were unable to detect the 18S rRNA gene sequence of the recently cultured *Algirosphaera robusta* [Medlin *et al.*, 2008; Probert *et al.*, 2007], despite the fact that this haptophyte represented a significant portion (~10–15%) of the calcareous nannofossil assemblage in some samples. The deep photic zone dwelling *Florisphaera profunda* [Principato *et al.*, 2006; Thomson *et al.*, 2004], estimated to represent 20–25% of the calcareous nannofossil composition in our core (Figure 7), was also not identified by the paleogenetic approach.

[38] On the other hand, the paleogenetic approach revealed more abundant sequences of noncalcifying species or those that were not previously described from nannofossil determination studies, including *Chrysochromulina* spp. (Figure 6) and, most notably, a potentially important environmental taxon represented by phylotype O as outlined in the next paragraph.

4.3. Using Fossil DNA to Estimate Paleoenvironmental Conditions During S1 Deposition

[39] The most striking observation from our paleogenetic data set is the dramatic shift in both dinoflagellate and haptophyte composition at ~44 cm (Figures 3 and 4). The timing of this ecological shift is synchronous with the disappearance of the fossil pentoliths of *Braarudosphaera bigelowii* (Figure 8), which has been previously defined as the beginning of “ecozone” C2 at 8 ¹⁴C kyr B.P. from other sapropel cores [Giunta et al., 2003; Principato et al., 2003].

[40] From the onset of S1 deposition (9.7 ¹⁴C kyr B.P.) until the ecological shift at ~8 kyr B.P., the fossil DNA stratigraphy recorded a predominance of dinoflagellate phylotype C with 100% sequence similarity to a predominant clone found in the anoxic, sulfidic sediments of the Black Sea (BS_DGGE_Euk8 [Coolen et al., 2006a]). Further studies are required to determine the geographic distribution of this phylotype, and whether it could be a potential marker for stratified and anoxic settings. If so, the predominance of phylotype C as well as a relatively constant C_{org} content of ~2 wt% (Figure 2) could be indicative of the presence of bottom water anoxia until ~8 ¹⁴C kyr B.P. at our coring site near the Nile fan at a depth of 1630 m. However, recent geochemical evidence showed that basin-wide only waters below 1800 m faced near to complete anoxia during S1 deposition [de Lange et al., 2008]. Since sedimentary DNA was extracted from two cm intervals, which represented roughly 200 years of deposition, we cannot rule out that occasional ventilation disrupted stratification and anoxia, and caused a periodic absence of phylotype C at this water depth, but these ventilation events did not last long enough to completely degrade labile compounds such as nucleic acids.

[41] Interval D-III (>44 cm; ~8–5.7 kyr B.P.; Figure 3) is marked by a different dinoflagellate community more related to clones recovered from marine surface waters and an absence or less predominant presence of phylotype C. This could be indicative of a reduced riverine input of freshwater and increasing sea surface salinities with newly formed oxygenated deep waters sinking more frequently to this depth than during early sapropel deposition [de Lange et al., 2008].

[42] According to the fossil DNA results, the haptophyte community in the eastern Mediterranean Sea until ~8 kyr B.P. was dominated by a haptophyte species (Phylotype O) with 99.5% sequence similarity to uncultivated haptophytes that, according to RNA stable isotopic probing (RNA-SIP) experiments, were capable of mixotrophic growth as predators of picocyanobacteria [Frias-Lopez et al., 2009]. The adoption of mixotrophy offers a survival strategy under oligotrophic oceanic conditions [Raven, 1997]. For example, Arenovski et al. [1995] presented experimental evidence of a decrease in the abundance of mixotrophic phototrophs under nutrient enrichment conditions, suggesting that phagotrophy

is used under low nutrient concentrations. Whether the haptophyte represented by phylotype O was indeed involved in phagotrophy during oligotrophic conditions in the Holocene eastern Mediterranean Sea is solely based on its high 18S rRNA gene sequence similarities and therefore speculative, but evidence for the presence of oligotrophic surface waters during early S1 deposition was also provided from fossil nannofossil compositions [e.g., Principato et al., 2006]. These studies showed a marked increase in paleofluxes of *Florisphaera profunda* coupled with a decrease in the accumulation rate of upper- and middle photic zone coccoliths, suggesting an ecological depth separation of the water column, probably characterized by higher nutrient availability at depth and nutrient-depleted surface waters during early to mid S1 formation [Principato et al., 2006].

4.4. Potential Use of Paleogenetics in Improving U₃₇^k-Paleothermometry

[43] Haptophyte algae are important to paleoceanographers because of the use of their specific alkenones in reconstructing sea surface temperature [Prahl and Wakeham, 1987]. As different species of haptophytes have a different functional response to growth temperature and thus a different U₃₇^k-temperature calibration [Prahl and Wakeham, 1987; Versteegh et al., 2001; Volkman et al., 1995], it is important for paleotemperature reconstructions to know which haptophyte species were present, and thus which calibration to apply. Previous studies have shown that fossil DNA enabled the identification of novel noncalcifying haptophytes as the major or only sources of fossil alkenones in less saline environments [Coolen et al., 2004b, 2006a, 2009; D'Andrea et al., 2006]. Our paleogenetics survey did not reveal any sequences related to noncalcifying alkenone sources, and based on the nannofossil composition in our core as well as cores analyzed by others [Negri et al., 2003; Principato et al., 2006], *E. huxleyi* is expected to have been the major source of alkenones during S1 deposition. We, therefore, did not find evidence for the need of a species-specific calibration of the alkenone-based SST estimates during S1 deposition. The SST values based on the general U₃₇^k calibration [Prahl and Wakeham, 1987] (Figure 2) are well within the range estimated for the sapropel S1 from other sediment cores from the eastern Mediterranean [Emeis et al., 2003].

5. Conclusion

[44] Despite the presence of low concentrations of lipid biomarkers diagnostic for dinoflagellates and haptophytes (i.e., dinosterol and long-chain alkenones), ~500 bp long 18S rDNA fragments of these protists could not be amplified by PCR in the C_{org}-depleted marls flanking the S1, thereby limiting the analysis of the relatively long fossil DNA fragments to the C_{org}-rich S1 sediments. None of the haptophytes present in the nannofossil assemblage or previously published dinoflagellates found as cysts could be positively identified in the C_{org}-rich S1 intervals using the fossil DNA approach. Instead, the fossil DNA approach was shown to be useful in identifying predominant and potentially important taxa that were not revealed by nannofossils or cysts. Our paleogenetic approach suggests a major shift in dinoflagellate and haptophyte populations during deposition of S1 at ~8 ¹⁴C kyr B.P. ago, which coincided with the timing of

previously reported changes in Holocene hydrologic regimes in the eastern Mediterranean. In the absence of identical sequences of cultivated species for data comparison, and because of the relatively conserved nature of the analyzed 18S rRNA gene, it remains difficult to positively identify the past source organisms at the species level. However, with an ever growing number of sequenced genomes and environmental metagenomic information, it will eventually become possible to identify and select genetic markers for accurate identification of past microbial communities at the species level. In order to enhance the detection of preserved fossil plankton DNA in older and/or a wider variety of sediments in general, we suggest to explore the use of massive parallel pyrotag sequencing [Amaral-Zettler *et al.*, 2009; Sogin *et al.*, 2006] of PCR-amplified short hypervariable regions of faster evolving molecular genetic markers in addition to the most frequently analyzed rather conserved ribosomal RNA genes.

[45] **Acknowledgments.** We would like to thank Alina Stadnitskaia, Shauna ni Flaithearta, and the captain of the R/V *Pelagia* for obtaining the core and subsequent subsampling on board of the ship. Marianne Baas, Jort Ossebaar, and Sanela Gusic are thanked for analytical assistance. This work was supported by grants and prizes from the Netherlands Organization for Scientific Research (NWO Open Competition grant 813.03.001 to M.J.L.C., NWO Pass2 grant to G.J.d.L., and the Spinoza prize to J.S.S.D.) as well as NSF-OCE Chemical Oceanography grant 0825020 to M.J.L.C.

References

- Amaral-Zettler, L. A., E. A. McCliment, H. W. Ducklow, and S. M. Huse (2009), A method for studying protistan diversity using massively parallel sequencing of V9 hypervariable regions of small-subunit ribosomal RNA genes, *PLoS ONE*, *4*(7), e6372, doi:10.1371/journal.pone.0006372.
- Arenovski, A. L., E. L. Lim, and D. A. Caron (1995), Mixotrophic nanoplankton in oligotrophic surface waters of the Sargasso Sea may employ phagotrophy to obtain major nutrients, *J. Plankton Res.*, *17*, 801–820, doi:10.1093/plankt/17.4.801.
- Bethoux, J. P. (1993), Mediterranean sapropel formation, dynamic and climatic viewpoints, *Oceanol. Acta*, *16*, 127–133.
- Bissett, A., J. A. E. Gibson, S. N. Jarman, K. M. Swadling, and L. Cromer (2005), Isolation, amplification, and identification of ancient copepod DNA from lake sediments, *Limnol. Oceanogr. Methods*, *3*, 533–542.
- Boere, A. C., B. Abbas, W. I. C. Rijpstra, G. J. M. Versteegh, J. K. Volkman, J. S. Sinninghe Damsté, and M. J. L. Coolen (2009), Late-Holocene succession of dinoflagellates in an Antarctic fjord using a multi-proxy approach: Paleo-environmental genomics, lipid biomarkers and palynomorphs, *Geobiology*, *7*, 265–281, doi:10.1111/j.1472-4669.2009.00202.x.
- Boon, J. J., W. I. C. Rijpstra, F. de Lange, J. W. de Leeuw, M. Yoshioka, and Y. Shimizu (1979), Black sea sterol—A molecular fossil for dinoflagellate blooms, *Nature*, *277*, 125–127, doi:10.1038/277125a0.
- Brassell, S. C., G. Eglinton, I. T. Marlowe, U. Pflaumann, and M. Sarnthein (1986), Molecular stratigraphy: A new tool for climatic assessment, *Nature*, *320*, 129–133, doi:10.1038/320129a0.
- Calvert, S. E. (1983), Geochemistry of Pleistocene sapropels and associated sediments from the eastern Mediterranean, *Oceanol. Acta*, *6*, 255–267.
- Casford, J. S. L., E. J. Rohling, R. H. Abu-Zied, C. Fontanier, F. J. Jorissen, M. J. Leng, G. Schmiedl, and J. Thomson (2003), A dynamic concept for eastern Mediterranean circulation and oxygenation during sapropel formation, *Palaeogeogr. Palaeoclimatol. Palaeoecol.*, *190*, 103–119, doi:10.1016/S0031-0182(02)00601-6.
- Castradori, D. (1993), Calcareous nannofossils and the origin of eastern Mediterranean sapropels, *Paleoceanography*, *8*, 459–471, doi:10.1029/93PA00756.
- Cheddadi, R., and M. Rossignol-Strick (1995), Improved preservation of organic matter and pollen in eastern Mediterranean sapropels, *Paleoceanography*, *10*, 301–309, doi:10.1029/94PA02673.
- Coolen, M. J. L., and J. Overmann (1998), Analysis of subfossil molecular remains of purple sulfur bacteria in a lake sediment, *Appl. Environ. Microbiol.*, *64*, 4513–4521.
- Coolen, M. J. L., and J. Overmann (2007), 217 000-year-old DNA sequences of green sulfur bacteria in Mediterranean sapropels and their implications for the reconstruction of the paleoenvironment, *Environ. Microbiol.*, *9*, 238–249, doi:10.1111/j.1462-2920.2006.01134.x.
- Coolen, M. J. L., E. C. Hopmans, W. I. C. Rijpstra, G. Muyzer, S. Schouten, J. K. Volkman, and J. S. Sinninghe Damsté (2004a), Evolution of the methane cycle in Ace Lake (Antarctica) during the Holocene: Response of methanogens and methanotrophs to environmental change, *Org. Geochem.*, *35*, 1151–1167, doi:10.1016/j.orggeochem.2004.06.009.
- Coolen, M. J. L., G. Muyzer, W. I. C. Rijpstra, S. Schouten, J. K. Volkman, and J. S. Sinninghe Damsté (2004b), Combined DNA and lipid analyses of sediments reveal changes in Holocene haptophyte and diatom populations in an Antarctic lake, *Earth Planet. Sci. Lett.*, *223*, 225–239, doi:10.1016/j.epsl.2004.04.014.
- Coolen, M. J. L., A. Boere, B. Abbas, M. Baas, S. G. Wakeham, and J. S. Sinninghe Damsté (2006a), Ancient DNA derived from alkenone-biosynthesizing haptophytes and other algae in Holocene sediments from the Black Sea, *Paleoceanography*, *21*, PA1005, doi:10.1029/2005PA001188.
- Coolen, M. J. L., G. Muyzer, S. Schouten, J. K. Volkman, and J. S. Sinninghe Damsté (2006b), Sulfur and methane cycling during the Holocene in Ace Lake (Antarctica) revealed by lipid and DNA stratigraphy, in *Past and Present Water Column Anoxia*, pp. 41–65, Springer, Dordrecht, Netherlands, doi:10.1007/1-4020-4297-3_03.
- Coolen, M. J. L., J. K. Volkman, B. Abbas, G. Muyzer, S. Schouten, and J. S. Sinninghe Damsté (2007), Identification of organic matter sources in sulfidic late Holocene Antarctic fjord sediments from fossil rDNA sequence analysis, *Paleoceanography*, *22*, PA2211, doi:10.1029/2006PA001309.
- Coolen, M. J. L., H. M. Talbot, B. A. Abbas, C. Ward, S. Schouten, J. K. Volkman, and J. S. Sinninghe Damsté (2008), Sources for sedimentary bacteriohopanepolyols as revealed by 16S rDNA stratigraphy, *Environ. Microbiol.*, *10*, 1783–1803, doi:10.1111/j.1462-2920.2008.01601.x.
- Coolen, M. J. L., J. P. Saenz, L. Giosan, N. Y. Trowbridge, P. Dimitrov, D. Dimitrov, and T. I. Eglinton (2009), DNA and lipid molecular stratigraphic records of haptophyte succession in the Black Sea during the Holocene, *Earth Planet. Sci. Lett.*, *284*, 610–621, doi:10.1016/j.epsl.2009.05.029.
- Corinaldesi, C., F. Beolchini, and A. Dell'Anno (2008), Damage and degradation rates of extracellular DNA in marine sediments: Implications for the preservation of gene sequences, *Mol. Ecol.*, *17*, 3939–3951, doi:10.1111/j.1365-294X.2008.03880.x.
- Crudeli, D., J. R. Young, E. Erba, G. J. de Lange, K. Henriksen, H. Kinkel, C. P. Slomp, and P. Ziveri (2004), Abnormal carbonate diagenesis in Holocene-late Pleistocene sapropel-associated sediments from the eastern Mediterranean; evidence from *Emiliania huxleyi* coccolith morphology, *Mar. Micropaleontol.*, *52*, 217–240, doi:10.1016/j.marmicro.2004.04.010.
- D'Andrea, W. J., M. Lage, J. B. H. Martiny, A. D. Laatsch, L. A. Amaral-Zettler, M. L. Sogin, and Y. Huang (2006), Alkenone producers inferred from well-preserved 18S rDNA in Greenland lake sediments, *J. Geophys. Res.*, *111*, G03013, doi:10.1029/2005JG000121.
- de Lange, G. J., and H. L. ten Haven (1983), Recent sapropel formation in the eastern Mediterranean, *Nature*, *305*, 797–798, doi:10.1038/305797a0.
- de Lange, G. J., J. Thomson, A. Reitz, C. P. Slomp, M. S. Principato, E. Erba, and C. Corselli (2008), Synchronous basin-wide formation and redox-controlled preservation of a Mediterranean sapropel, *Nat. Geosci.*, *1*, 606–610, doi:10.1038/ngeo283.
- Diez, B., C. Pedrós-Alió, T. L. Marsh, and R. Massana (2001), Application of denaturing gradient gel electrophoresis (DGGE) to study the diversity of marine picoeukaryotic assemblages and comparison of DGGE with other molecular techniques, *Appl. Environ. Microbiol.*, *67*, 2942–2951, doi:10.1128/AEM.67.7.2942-2951.2001.
- Edwardsen, B., W. Eikrem, J. C. Green, R. A. Andersen, S. Moon-van der Staay, and L. K. Medlin (2000), Phylogenetic reconstructions of the Haptophyta inferred from 18S ribosomal DNA sequences and available morphological data, *Phycologia*, *39*, 19–35, doi:10.2216/i0031-8884-39-1-19.1.
- Emeis, K.-C., *et al.* (2003), Eastern Mediterranean surface water temperatures and $\delta^{18}\text{O}$ composition during deposition of sapropels in the late Quaternary, *Paleoceanography*, *18*(1), 1005, doi:10.1029/2000PA000617.
- Frada, M., F. Not, I. Probert, and C. de Vargas (2006), CaCO_3 optical detection with fluorescent in situ hybridization: A new method to identify and quantify calcifying microorganisms from the oceans, *J. Phycol.*, *42*, 1162–1169, doi:10.1111/j.1529-8817.2006.00276.x.
- Frias-Lopez, J., A. Thompson, J. Waldbauer, and S. W. Chisholm (2009), Use of stable isotope-labelled cells to identify active grazers of picocyanobacteria in ocean surface waters, *Environ. Microbiol.*, *11*, 512–525, doi:10.1111/j.1462-2920.2008.01793.x.
- Gennari, G., F. Tamburini, D. Ariztegui, I. Hajdas, and S. Spezzaferri (2009), Geochemical evidence for high-resolution variations during deposition of the Holocene S1 sapropel on the Cretan Ridge, eastern

- Mediterranean, *Palaeogeogr. Palaeoclimatol. Palaeoecol.*, *273*, 239–248, doi:10.1016/j.palaeo.2008.06.007.
- Giunta, S., A. Negri, C. Morigi, L. Capotondi, N. Combourieu-Nebout, K. C. Emeis, F. Sangiorgi, and L. Vigliotti (2003), Coccolithophorid ecostratigraphy and multi-proxy paleoceanographic reconstruction in the Southern Adriatic Sea during the last deglacial time (Core AD91-17), *Palaeogeogr. Palaeoclimatol. Palaeoecol.*, *190*, 39–59, doi:10.1016/S0031-0182(02)00598-9.
- Godhe, A., M. E. Asplund, K. Harnstrom, V. Saravanan, A. Tyagi, and I. Karunasagar (2008), Quantification of diatom and dinoflagellate biomasses in coastal marine seawater samples by real-time PCR, *Appl. Environ. Microbiol.*, *74*, 7174–7182, doi:10.1128/AEM.01298-08.
- Harvey, H. R., S. A. Bradshaw, S. C. M. O'Hara, G. Eglinton, and E. D. S. Corner (1988), Lipid composition of the marine dinoflagellate *Scrippsiella Trochoidea*, *Phytochemistry*, *27*, 1723–1729, doi:10.1016/0031-9422(88)80432-1.
- Head, M. J. (1996), Modern dinoflagellate cysts and their biological affinities, in *Palynology: Principles and Applications*, pp. 1197–1248, Am. Assoc. of Stratigr. Palynol. Found., Salt Lake City, Utah.
- Kidd, R. B., M. B. Cita, and W. B. F. Ryan (1978), Stratigraphy of eastern Mediterranean sapropel sequences recovered during DSDP leg 42A and their paleoenvironmental significance, *Initial Rep. Deep Sea Drill. Proj.*, *42*, 421–443.
- LaJeunesse, T. C., G. Lambert, R. A. Andersen, M. A. Coffroth, and D. W. Galbraith (2005), *Symbiodinium* (Pyrrophyta) genome sizes (DNA content) are smallest among dinoflagellates, *J. Phycol.*, *41*, 880–886, doi:10.1111/j.0022-3646.2005.04231.x.
- Lindahl, T. (1993), Instability and decay of the primary structure of DNA, *Nature*, *362*, 709–715, doi:10.1038/362709a0.
- Ludwig, W., et al. (2004), ARB: A software environment for sequence data, *Nucleic Acids Res.*, *32*, 1363–1371, doi:10.1093/nar/gkh293.
- Manske, A. K., U. Henßge, J. Glaeser, and J. Overmann (2008), Subfossil 16S rRNA gene sequences of green sulfur bacteria in the Black Sea and their implications for past photic zone anoxia, *Appl. Environ. Microbiol.*, *74*, 624–632, doi:10.1128/AEM.02137-07.
- Mansour, M. P., J. K. Volkman, and S. I. Blackburn (2003), The effect of growth phase on the lipid class, fatty acid and sterol composition in the marine dinoflagellate, *Gymnodinium sp.* in batch culture, *Phytochemistry*, *63*, 145–153, doi:10.1016/S0031-9422(03)00052-9.
- Marlowe, I. T., J. C. Green, A. C. Neal, S. C. Brassell, G. Eglinton, and P. A. Course (1984), Long-Chain ($n-C_{37}$ – C_{39}) alkenones in the Prymnesiophyceae. Distribution of alkenones and other lipids and their taxonomic significance, *Br. Phycol. J.*, *19*, 203–216, doi:10.1080/00071618400650221.
- Medlin, L., H. J. Elwood, S. Stickel, and M. L. Sogin (1988), The characterization of enzymatically amplified eukaryotic 16S-like rRNA-coding regions, *Gene*, *71*, 491–499, doi:10.1016/0378-1119(88)90066-2.
- Medlin, L. K., A. G. Sáez, and J. R. Young (2008), A molecular clock for coccolithophores and implications for selectivity of phytoplankton extinctions across the K/T boundary, *Mar. Micropaleontol.*, *67*, 69–86, doi:10.1016/j.marmicro.2007.08.007.
- Meier, K. J. S., K. A. F. Zonneveld, S. Kasten, and H. Willems (2004), Different nutrient sources forcing increased productivity during eastern Mediterranean S1 sapropel formation as reflected by calcareous dinoflagellate cysts, *Paleoceanography*, *19*, PA1012, doi:10.1029/2003PA000895.
- Moodley, L., J. J. Middelburg, P. M. J. Herman, K. Soetaert, and G. J. de Lange (2005), Oxygenation and organic-matter preservation in marine sediments: Direct experimental evidence from ancient organic carbon-rich deposits, *Geology*, *33*, 889–892, doi:10.1130/G21731.1.
- Mouradian, M., R. J. Panetta, A. de Vernal, and Y. Gélinais (2007), Dinosterols or dinocysts to estimate dinoflagellate contributions to marine sedimentary organic matter? *Limnol. Oceanogr.*, *52*, 2569–2581, doi:10.4319/lo.2007.52.6.2569.
- Muyzer, G., E. C. de Waal, and A. G. Uitterlinden (1993), Profiling of complex microbial populations by denaturing gradient gel electrophoresis analysis of polymerase chain reaction-amplified genes coding for 16S rRNA, *Appl. Environ. Microbiol.*, *59*, 695–700.
- Negri, A., and S. Giunta (2001), Calcareous nannofossil paleoecology in the sapropel S1 of the eastern Ionian sea: Paleoceanographic implications, *Palaeogeogr. Palaeoclimatol. Palaeoecol.*, *169*, 101–112, doi:10.1016/S0031-0182(01)00219-X.
- Negri, A., C. Morigi, and S. Giunta (2003), Are productivity and stratification important to sapropel deposition? Microfossil evidence from late Pliocene insolation cycle 180 at Vrica, Calabria, *Palaeogeogr. Palaeoclimatol. Palaeoecol.*, *190*, 243–255, doi:10.1016/S0031-0182(02)00608-9.
- Not, F., R. Gausling, F. Azam, J. F. Heidelberg, and A. Z. Worden (2007), Vertical distribution of picoeukaryotic diversity in the Sargasso Sea, *Environ. Microbiol.*, *9*, 1233–1252, doi:10.1111/j.1462-2920.2007.01247.x.
- Passier, H. F., J. J. Middelburg, B. J. H. van Os, and G. J. de Lange (1996), Diagenetic pyritisation under eastern Mediterranean sapropels caused by downward sulphide diffusion, *Geochim. Cosmochim. Acta*, *60*, 751–763, doi:10.1016/0016-7037(95)00419-X.
- Prahl, F. G., and S. G. Wakeham (1987), Calibration of unsaturation patterns in long-chain ketone compositions for palaeotemperature assessment, *Nature*, *330*, 367–369, doi:10.1038/330367a0.
- Principato, M. S., S. Giunta, C. Corselli, and A. Negri (2003), Late Pleistocene-Holocene planktonic assemblages in three box-cores from the Mediterranean Ridge area (west-southwest of Crete): Palaeoecological and palaeoceanographic reconstruction of sapropel S1 interval, *Palaeogeogr. Palaeoclimatol. Palaeoecol.*, *190*, 61–77, doi:10.1016/S0031-0182(02)00599-0.
- Principato, M. S., D. Crudeli, P. Ziveri, C. P. Slomp, C. Corselli, E. Erba, and G. J. de Lange (2006), Phyto- and zooplankton paleofluxes during the deposition of sapropel S1 (eastern Mediterranean): Biogenic carbonate preservation and paleoecological implications, *Palaeogeogr. Palaeoclimatol. Palaeoecol.*, *235*, 8–27, doi:10.1016/j.palaeo.2005.09.021.
- Probert, I., J. Fresnel, C. Billard, M. Geisen, and J. R. Young (2007), Light and electron microscope observations of *Algirosphaera robusta* (Prymnesiophyceae), *J. Phycol.*, *43*, 319–332, doi:10.1111/j.1529-8817.2007.00324.x.
- Pruesse, E., C. Quast, K. Knittel, B. M. Fuchs, W. G. Ludwig, J. Peplies, and F. O. Glöckner (2007), SILVA: A comprehensive online resource for quality checked and aligned ribosomal RNA sequence data compatible with ARB, *Nucleic Acids Res.*, *35*, 7188–7196, doi:10.1093/nar/gkm864.
- Raven, J. A. (1997), Phagotrophy in phototrophs, *Limnol. Oceanogr.*, *42*, 198–205, doi:10.4319/lo.1997.42.1.0198.
- Reitz, A., and G. J. de Lange (2006), Abundant Sr-rich aragonite in eastern Mediterranean sapropel S1: Diagenetic vs. detrital/biogenic origin, *Palaeogeogr. Palaeoclimatol. Palaeoecol.*, *235*, 135–148, doi:10.1016/j.palaeo.2005.10.024.
- Reitz, A., J. Thomson, G. J. de Lange, and C. Hensen (2006), Source and development of large manganese enrichments above eastern Mediterranean sapropel S1, *Paleoceanography*, *21*, PA3007, doi:10.1029/2005PA001169.
- Robinson, N., G. Eglinton, S. C. Brassell, and P. A. Cranwell (1984), Dinoflagellate origin for sedimentary 4α -methylsteroids and $5\alpha(H)$ -stanols, *Nature*, *308*, 439–442, doi:10.1038/308439a0.
- Roether, W., and R. Well (2001), Oxygen consumption in the eastern Mediterranean, *Deep Sea Res., Part I*, *48*, 1535–1551, doi:10.1016/S0967-0637(00)00102-3.
- Rohling, E. J. (1989), Late Quaternary changes in Mediterranean intermediate water density and formation rate, *Paleoceanography*, *4*, 531–545, doi:10.1029/PA004i005p00531.
- Rohling, E. J., and R. C. Thunell (1999), Five decades of Mediterranean palaeoclimate and sapropel studies, *Mar. Geol.*, *153*, 7–10, doi:10.1016/S0025-3227(98)00093-0.
- Rontani, J.-F., B. Bekker, and J. K. Volkman (2004), Long-chain alkenones and related compounds in the benthic haptophyte *Chrysothila lamellosa* Anand HAP 17, *Phytochemistry*, *65*, 117–126, doi:10.1016/j.phytochem.2003.09.021.
- Sangiorgi, F., D. Fabbri, M. Comandini, G. Gabbianelli, and E. Tagliavini (2005), The distribution of sterols and organic-walled dinoflagellate cysts in surface sediments of the North-western Adriatic Sea (Italy), *Estuarine Coastal Shelf Sci.*, *64*, 395–406, doi:10.1016/j.ecss.2005.03.005.
- Schloss, P. D., and J. Handelsman (2005), Introducing DOTUR, a computer program for defining operational taxonomic units and estimating species richness, *Appl. Environ. Microbiol.*, *71*, 1501–1506, doi:10.1128/AEM.71.3.1501-1506.2005.
- Skovgaard, A. (2005), Infection with the dinoflagellate parasite *Blastodinium* spp. in two Mediterranean copepods, *Aquat. Microb. Ecol.*, *38*, 93–101, doi:10.3354/ame038093.
- Skovgaard, A., R. Massana, and E. Saiz (2007), Parasitic species of the genus *Blastodinium* (Blastodiniophyceae) are peridinioid dinoflagellates, *J. Phycol.*, *43*, 553–560, doi:10.1111/j.1529-8817.2007.00338.x.
- Sogin, M. L., H. G. Morrison, J. A. Huber, D. M. Welch, S. M. Huse, P. R. Neal, J. M. Arrieta, and G. J. Herndl (2006), Microbial diversity in the deep sea and the underexplored “rare biosphere”, *Proc. Natl. Acad. Sci. U. S. A.*, *103*, 12,115–12,120, doi:10.1073/pnas.0605127103.
- Tamura, K., J. Dudley, M. Nei, and S. Kumar (2007), MEGA4: Molecular evolutionary genetics analysis (MEGA) software version 4.0, *Mol. Biol. Evol.*, *24*, 1596–1599, doi:10.1093/molbev/msm092.
- Thomson, J., D. Mercione, G. J. de Lange, and P. J. M. van Santvoort (1999), Review of recent advances in the interpretation of eastern Mediterranean sapropel S1 from geochemical evidence, *Mar. Geol.*, *153*, 77–89, doi:10.1016/S0025-3227(98)00089-9.
- Thomson, J., D. Crudeli, G. J. de Lange, C. P. Slomp, E. Erba, C. Corselli, and S. E. Calvert (2004), *Florisphaera profunda* and the origin and diagenesis of carbonate phases in eastern Mediterranean sapropel units, *Paleoceanography*, *19*, PA3003, doi:10.1029/2003PA000976.

- Versteegh, G. J. M., R. Riegman, J. W. de Leeuw, and J. H. F. Jansen (2001), U_{37}^K values for *Isochrysis galbana* as a function of culture temperature, light intensity and nutrient concentrations, *Org. Geochem.*, 32, 785–794, doi:10.1016/S0146-6380(01)00041-9.
- Volkman, J. K. (2003), Sterols in microorganisms, *Appl. Microbiol. Biotechnol.*, 60, 495–506.
- Volkman, J. K., S. M. Barrett, S. I. Blackburn, and E. L. Sikes (1995), Alkenones in *Gephyrocapsa oceanica*: Implications for studies of paleoclimate, *Geochim. Cosmochim. Acta*, 59, 513–520, doi:10.1016/0016-7037(95)00325-T.
- Volkman, J. K., S. M. Barrett, S. I. Blackburn, M. P. Mansour, E. L. Sikes, and F. Gelin (1998), Microalgal biomarkers: A review of recent research developments, *Org. Geochem.*, 29, 1163–1179, doi:10.1016/S0146-6380(98)00062-X.
- Zonneveld, K. A. F., G. J. M. Versteegh, and G. J. de Lange (2001), Palaeoproductivity and post-depositional aerobic organic matter decay reflected by dinoflagellate cyst assemblages of the eastern Mediterranean S1 sapropel, *Mar. Geol.*, 172, 181–195, doi:10.1016/S0025-3227(00)00134-1.
- Zonneveld, K. A. F., G. J. M. Versteegh, and M. Kodrans-Nsiah (2008), Preservation and organic chemistry of Late Cenozoic organic-walled dinoflagellate cysts: A review, *Mar. Micropaleontol.*, 68, 179–197, doi:10.1016/j.marmicro.2008.01.015.
-
- A. C. Boere, W. I. C. Rijpstra, and J. S. Sinninghe Damsté, Department of Marine Organic Biogeochemistry, NIOZ Royal Netherlands Institute for Sea Research, PO Box 59, NL-1790 AB Den Burg, Netherlands. (arjan.boere@nioz.nl)
- M. J. L. Coolen, Department of Marine Chemistry and Geochemistry, Woods Hole Oceanographic Institution, 360 Woods Hole Rd., MS#4, Woods Hole, MA 02543, USA.
- G. J. de Lange, Faculty of Earth Sciences, Utrecht University, PO Box 80.021, NL-3508 TA Utrecht, Netherlands.
- E. Malinverno, Department of Geological Sciences and Geotechnologies, University of Milan-Bicocca, Piazza della Scienza 4, I-20126 Milano, Italy.